UNIVERSITY OF LEICESTER

GY7705

Scientific Report

Student: Satyam Shah

CW1

School of Geography, Geology and the Environment Sciences

University of Leicester

December 2024

Table of Contents

Utilising Remote Sensing application techniques to assess 25-Year Land use/Land cover (LULC) temporal dynamics of Kathmandu city, Nepal.

1. Introduction

Over the past few decades, the land use and land cover (LULC) changes has emerged as a global critical concern due to its rapid rate and magnitude at which it is observed resulting in far reaching environmental consequences (Jarnagin, 2013). This accelerated transformational change has been attributed to trigger multiple cascading impact across multiple facets on this planet. The repercussions consist of change in climate patterns, biodiversity extinction, habitat loss, rapid population growth, drought and many more. Recent studies suggest the primary driver of this alteration is rapid urbanization, given the scale and rate with which it is being evidenced mainly across developing nations, as opposed to developed nations due to the prevalence of sudden surge in population growth (Roy et al., 2022). The rural and developing regions experience greater growth uncertainties that often leads to challenges in anticipating the urbanisation pattern, however the current prediction indicate; by 2030 an approximate 40% of world's population is projected to reside in urban areas where majority of that predicted population figure is expected to originate from developing or rural regions (Seto et al., 2012; Mahmoudzadeh, 2022). The unorganised expansion of population during urbanization ultimately results in sprawl due to lack of infrastructure planning and ability to meet the residential demands, resulting in coerced conversion of valuable arable lands or forest to utility and residential services within the urban setting (Mahmoudzadeh, 2022). With this shift in dynamics of LULC, the world is brought to experience the importance and need to understand such complex change in patterns and its implications (Hailu et al., 2020). Thus, the role of remote sensing application in assessing LULC change is vital in order to address unorganised urban expansion, illegal forest logging, monitoring water bodies, agricultural lands and various interconnected ecosystems (Hailu et al., 2020; Jarnagin, 2013). Hence, this report aims to analyse and assess LULC changes in Kathmandu city, Nepal over a 25-year period with a particular emphasis on urban sprawl.

1.1 RS Utility for Land Use and Land Cover (LULC)

In the recent years, the applicability of satellite imageries utilising remote sensing techniques have shown significant advancements in addressing multiple intertwined environmental issues associated with LULC as it provides multi-temporal insights critical in assessing change (Rogan and Chen, 2015). While various existing conventional techniques such as ground or field-based surveying is prone to under sampling, spatial biases and lack capabilities to inscribe big temporal LULC changes over prolonged timeframes, the utilisation of historical Landsat archived data have enabled to generate estimates and further evaluation of LULC trends. Muriithi's (2016) 25-year study on semi-arid watersheds of Laikipia, Kenya demonstrates how spatial pockets of forest diminish with extreme commercial horticulture due to socio-economic factors. Likewise, Weng's (2010) evaluation on urban expansion of Zhujiang Delta, China highlights a key consequence of unorganised urban expansion (i.e., increase in radiant temperature of 13.01K). Nichol (1994) also documented the difference in mesoscale temperatures across housing estates in Singapore to examine LULC urban induced change in surface temperature. Fenta et al., (2017) investigation on three decadal urban dynamics of Mekelle city in Ethiopia shows how 88% of urban expansion occurred at the expense of agricultural

land between 1984-2014. (Khamphilung et al., 2023) conducted a study on flood event detection at North-eastern Thailand utilising Sentinel-1 SAR-C data and machine learning classifiers to quantify the susceptibility of LULC demonstrating the best utility of remote sensing in comprehending LULC trends. Similarly, (Dutta et al., 2018) 25-year analysis on land use patterns using Landsat4-5 TM and 8 TIRS revealed the development of heat island effect across Durgapur, Eastern India where conversion of 77% of vegetation was observed being attributed to build up along with an added 1.4% increase in land surface temperature (LST) annually. Several studies also suggest the vitality of remote sensing techniques in LULC when tracing rates of urban epidemiology, a study by Derdouri et al., (2021) highlights the correlation between change in LULC and surface heat island in inducing public health risks. A study by Muhammad et al., (2022) reveals the use of Cellular Automata Artificial Neural Networks (CA-ANN) and Multi-Criteria Evaluation (MCE) to detect LULC from 1990-2020 in Linyi city, China where impervious surfaces previously increased greatly from 10.48% - 27.93%, moreover the use of CA-ANN model now predicts the future increment rate of 40% for impervious surfaces by 2050 and decline of green spaces by 10% attributed to intense urban development in coming years. In contrast to the proven potency of remote sensing techniques in assessing LULC, it provides a budget efficient and time reducing alternative to other conventional methods that require greater manpower and costs, ultimately positioning computer processing of satellite imagery a feasible choice (Chagarlamudi and Plunkett, 2007).

1.2 Aims and Objectives

The key objectives of this research include:

I. To recognize and classify major LULC categories present in the study area, with a specific emphasis on decoding transitions from rural to urban regions.
II. To develop a time series(temporal) LULC map across a 25-year span (i.e., 1999 to 2024).
III. To analyse and detect any spatial and temporal patterns of classified LULC categories.
IV. To quantify and characterise the extent of urban sprawl within the study area between 1999 and 2024.
V. To perform a comprehensive accuracy assessment and assess the reliability of the LULC classification outcomes.
VI. To quantify and detect rates of change for each LULC classes.

2. Materials and Methods

2.1 Study site

The study is focused on Kathmandu, the capital city of Nepal situated between latitudes 27°40’N and 27°45’N and longitudes 85°16'E and 85°22'E (Paudyal et al., 2013). As illustrated in Figure 1, the right map emphasizes Kathmandu metropolitan city within Nepal on a wider geographical context while left inset map particularly shows Kathmandu city as the study area. This metropolitan city is situated within a bowl-shaped valley surrounded by the Mahabharat Range (i.e., Himalayan mountains), at an elevation level of 1,400m above sea-level (Zurick, 2010a). The city falls within a temperate broadleaf and mixed forest ecoregion being characterised by temperate climate and defined seasonal cycle of dry and wet phases (Zurick, 2010b). Since, the city lies within a valley, the land is known for its

fertility due to sediments formed by ancient lakes, thereby also fostering extensive agriculture for decades (Ross et al., 2008). Kathmandu is also prominently known for being the largest urban, political and economic focal point in all over Nepal (Thapa and Muryama, 2010; Timsina 2020). According to (Ishtiaque et al., 2017) the city widely thrived as an agricultural hub, but accelerated urbanization and population growth has induced significant conversion and LULC changes. Based on census data, the population growth of Kathmandu was recorded as 671,846 in 2001, further renumeration in 2021 revealed 1,442,271 in a span of 20 years (Subedi, 2014a). This unprecedented sudden surge in urban expansion at an annual rate of 4.02% and LULC conversions as evident by historical figures marks the city as an ideal area to conduct a LULC temporal study and comprehend further urban expansion patterns (Subedi, 2014b).

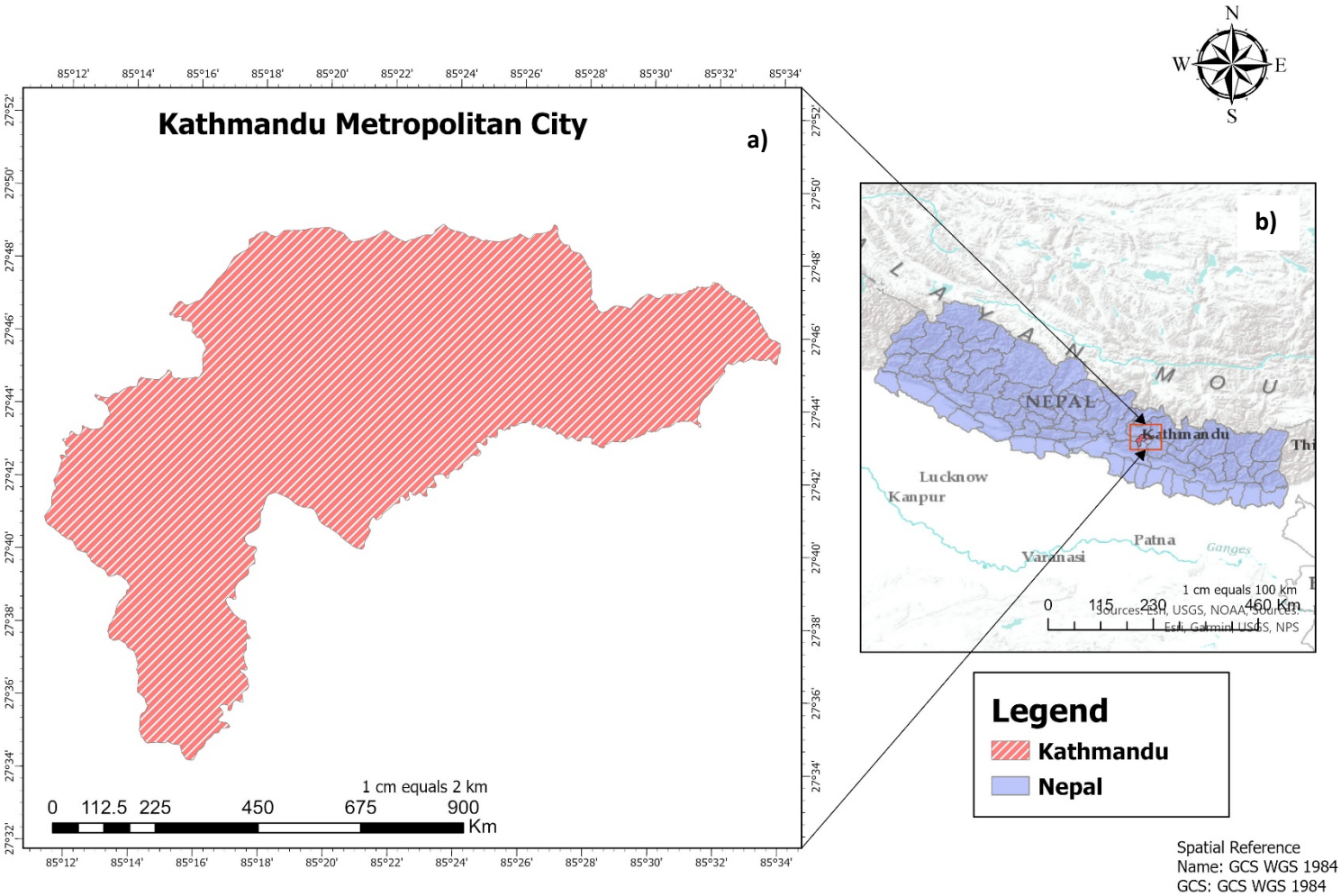

Figure 1: The inset panel(a) map on the left indicates study area while panel(b) shows a wider geographical outline and context of Nepal.

2.2 Data Sources and Sensors Implementation

For this study, the Landsat images with 30m x 30m spatial resolution covering the Kathmandu metropolitan city was sourced from the United States Geological Survey (USGS, 2024). Two datasets from distinct time-period were incorporated to aid the analysis of change detection. The Landsat 4-5 TM image was used for the year 1999 and Landsat 8-9 OLI/TIRS for the year 2024 respectively. The decision to extract Landsat 4-5 TM and Landsat 8-9 OLI/TIRS data was done to maintain the cross-sensor compatibility between sensors and consistency in spatial resolution prior to performing any computations. In addition, the presence of 12-bit radiometric resolution in Landsat8-9 OLI/TIRS enable for 4,096 levels of brightness compared to 256 levels(8-bit) of Landsat 4-5 TM resulting in finer distinction of surface patterns specifically beneficial for LULC classifications (Morfitt et al., 2015a). The SWIR and NIR bands of Landsat 8-9 OLI also possess an improved signal-to-noise ratios, suited for optimal performance in analysing vegetation and land cover types. Additionally, Landsat 8-9 also possess a push-broom design that assists in reducing geometric distortions ensuring high precision and gaps (Morfitt et al., 2015b).

Table 1: Overview of employed Satellite data and sensors for the study

Landsat Image Type	Level	Sensor	Spatial Resolution	Bands Used	Date of Image Acquisition	Source	Scenic Cloud Cover
Landsat 4-5 C2	1	TM (Thematic Mapper)	30m	1=Blue 2=Green 3=Red 4=NIR 5=SWIR1 7=SWIR2	04/18/1999	USGS	6.85
Landsat 8-9 C2	1	OLI (Operational Land Imager)	30m	2= Blue 3=Green 4=Red 5=NIR 6=SWIR1 7=SWIR2	04/30/2024	USGS	1.95

The choice to acquire images of April was to ensure observation of optimal vegetation phenology, uniform seasonal conditions (i.e., spring) to reduce cloud coverage between images from the two dates ultimately leading to process clear consistent images (Gozalez-Sanpedro, 2008). Likewise, the decision to utilise particular bands as shown in the table was in order to adhere by their spectral coverage and mainly relevance to LULC comparability between the two sensors.

2.3 Satellite-Data analysis framework

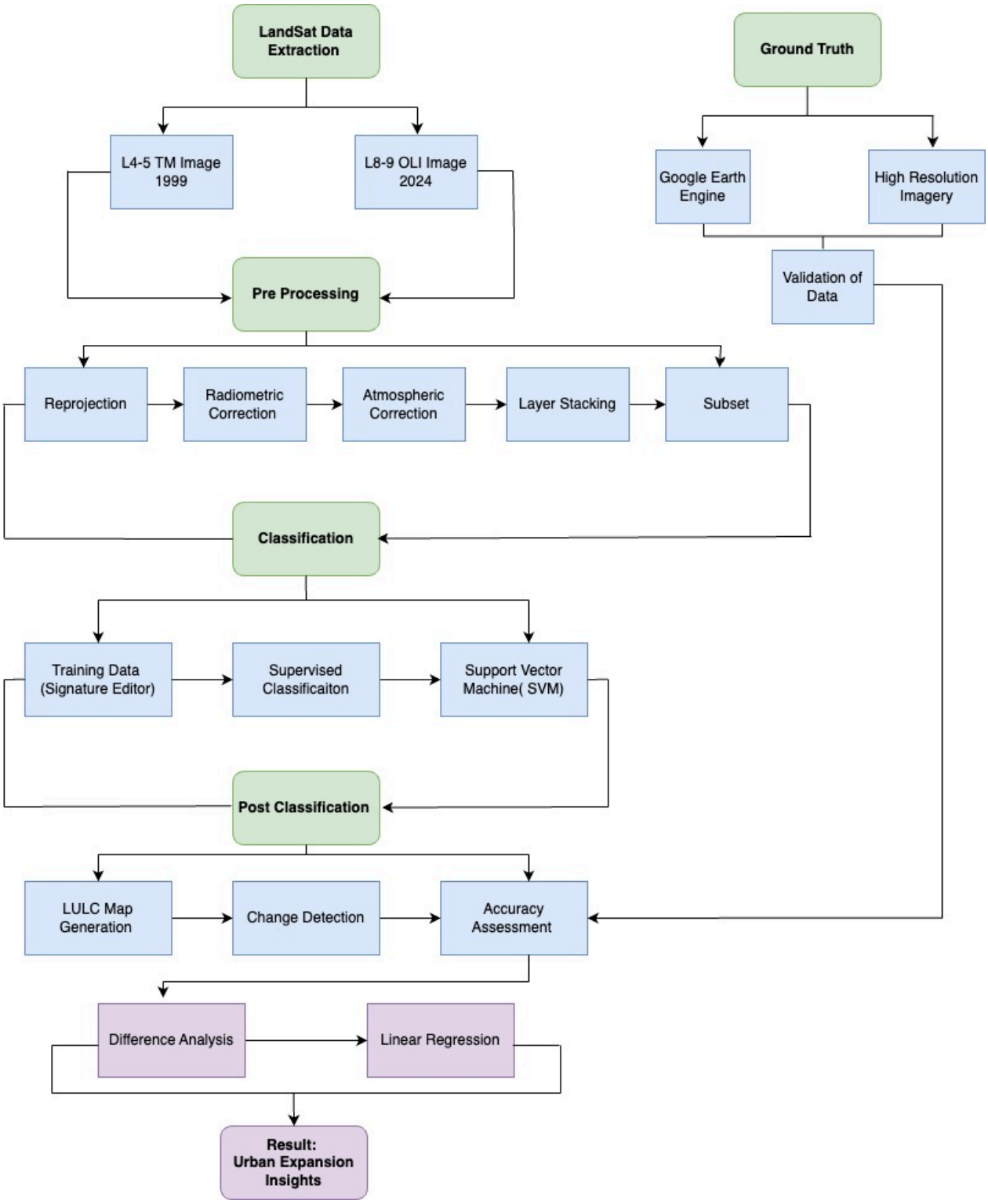

Figure 2: The schematic workflow diagram illustrates the methodologies utilised in the study.

2.3.1 Pre-processing

2.3.1.1 *Reprojection*

All Level 1 satellite band imageries used in the study were initially reprojected from UTM Zone 4NN to WGS84 coordinate system using ERDAS Imagine software to maintain the consistency, preserve features associated with edges of boundaries and prevent geometrical distortions.

2.3.1.2 *Radiometric Correction*

Radiometric corrections were applied onto individual bands to account for variation in solar angles. The sun elevation angle data was retrieved from the metadata in order to perform the correction where L_{corr} was referred to as corrected radiance, L_{raw} as raw radiance and ϑ_{sun} as sine of the sun elevation angle in degrees ultimately converted to radian for calculation $L_{corr} = L_{raw}/\sin(\vartheta_{sun})$. To apply the correction, the radiance of each pixel values was divided by sine of the sun elevation angle using the raster calculator tool to generate radiometrically correct band layers.

2.3.1.3 *Atmospheric Correction*

In order to enhance the accuracy of the surface reflectance values and acquire distortion free spectral signatures, the correction was achieved using DOS (Dark Object Subtraction) method. Initially, the minimum DN (Digital Number) values were determined from each band where pixel values were examined using histogram analysis on ERDAS Imagine. The minimum values were incorporated as haze correction factor in the formula $\rho = (DN - Haze) \times Gain$, where ρ represent surface reflectance, DN as raw digital number for each pixel and gain was set to 1 seamlessly removing all the scattering element from each band.

2.3.1.4 *Layer Stacking and Subsetting*

The layer stacking process involved combining individual spectral bands into a single composite multiband file to identify various features from the imagery prior to LULC classification. For Landsat 4-5TM, the band (Blue, Green, Red, NIR, SWIR1, SWIR2) were stacked while bands (Blue, Green, Red, NIR, SWIR1, SWIR2) were merged for Landsat 8-9 OLI/TIRS. The exclusion of certain bands from both satellite datasets were due to inapplicability to the AOI and study objectives. Subsequent to layer stacking, subset was clipped using vector boundary file based on the AOI from both pre-processed composites from 1999 and 2024. The subset process eliminated the post-processing time and promoted computational efficiency specific to the AOI.

2.3.2 Classification

Prior to the classification process, the LULC class establishment was validated using features observation from false composite bands, high resolution Google earth engine images and previous ground-based familiarity of the area. The LULC comprises of urban built up, dense forest, water bodies, fallow land and agriculture(Table 2). The training samples were acquired using the signature editor and polygon lasso tool based on particular reflectance properties to produce spectral signatures of LULC categories. The Support Vector Machine (SVM) algorithm under supervised

classification was applied to each image because of its capacity to process non-linear associations between spectral features and LULC classes known to be efficient, particularly in a heterogenous landscape like Kathmandu city.

2.3.3 Accuracy Assessment

To assess the accuracy of classifications, the results were incorporated onto ArcGIS Pro where a total of 180 stratified random pixels were derived for validation for both classified datasets. The assessment entailed cross checking the accuracy of assigned LULC classes on Goggle earth engine via overlaying accuracy points on high resolution imagery. To quantify the accuracy of LULC classes statistically, a confusion matrix was generated.

Table 2: LULC Class types and corresponding feature descriptions

LULC Class Type	Feature Composition
Water Bodies	Ponds, lakes, reservoirs, rivers and wetlands
Urban Built-up	Concrete buildings, Roads, industries, utility infrastructures, rooftops, asphalt paved areas and car park
Fallow Land	Grazed land, harvested land, resting cropland and tilled land
Agriculture	Crop cultivated fields, vineyards, orchards, pastureland and hay fields
Dense Forest	Closed canopy jungle, high density vegetation, large diameter trees, snags and downed logs

3. Results and Discussion

3.1 Interpretation of LULC classification outcomes

The classification findings of Kathmandu city satellite data display substantial LULC change transformations between the year 1999 to 2024 as shown in tables 3 and 4. The classified 1999 LULC product clearly highlights the spatial extent and predominance of agricultural land indicated in (yellow) , dense forest (green) and urban bult up (red) all compacted in one central region while source of water bodies (blue) and fallow land (orange) can be observed scattered across the valley, nonetheless occupying comparatively smaller proportions of the area.

Table 3: Land use/land cover transformation dynamics of Kathmandu between 1999 and 2024.

	1999		**2024**	
LULC Class	**Area (Km²)**	**%**	**Area (Km²)**	**%**
Water Bodies	25	6.06	10	2.41
Urban Built-up	20	4.84	161	38.89
Fallow Land	135	32.69	7	1.69
Agriculture	132	31.96	110	26.57
Dense Forest	101	24.46	126	30.43
Total	413	100	414	100

However, the 2024 LULC product reveals a striking progression and spread of urban built-up areas

infringed upon surrounding fallow and agricultural lands. Likewise, the urban sprawl pattern is distinctly pronounced in regions previously utilised as agricultural lands. Dense forests exhibit comparatively stable coverage, although some areas indicate to have undergone changes likely due to natural calamities such as soil erosion, landslides and urban settlements. The subtle change in forest is anticipated, given the nature of such recurring events in that topography. The water network can be observed being constrained by urban expansion also suggesting the conversion of urban infrastructure being built over the river lines. The major river lines and reservoirs still retain their presence.

3.2 LULC Change Analysis

As per the results, the analysis of LULC suggest a significant detection of change across most of the classified variables. The transformation within the last 25 years in Kathmandu city can be attributed to several anthropogenic factors, however, the findings suggest urban sprawl to be one major driver to have initiated this temporal shift and conversion among classified LULC classes. In 1999, the most prominent land cover classes were Agriculture 132 km² (31.96%) and fallow land 135 km² (32.69%) collectively consisting of over 64% total area. Dense forest areas covered 101 km² (24.46%) whereas urban settlements consisted just 20 km² (4.84%) coverage and water bodies accounted 25 km² (6.06%) respectively. By the year 2024, the LULC outline of Kathmandu can be observed experiencing striking transitions. The results reveal urban built-up to have surged from 20 km² in 1999 to 161 km² (38.89%) by 2024 which is an eight-fold increase indicative of rapid urbanization in a metropolis. This expansion can be attributed to have appeared at the cost of fallow land which reduced to 7 km² (1.69%) and agriculture plummeted to 100 km² (26.57%) in 2024. Regardless of reductions, dense forests appear to show resilience as it increased by 126 km² (30.43%) reflecting potential reforestation and natural forest regeneration phenomenon. Contrastingly, the regions that were previously occupied by water sources reduced by almost over half (i.e., 25 km², 6.06%) to 10 km² (2.42%) indicating pressures on water bodies due to urban encroachments and changes in land use.

Table 4: 25-Year LULC Change Matrix of Kathmandu city: Absolute and Relative Changes (1999-2024)

LULC Class	Area (Km²) in 1999	Area (Km²) in 2024	Change in Area (Km²)	% Change
Water Bodies	25	10	-15	-60.00%
Urban Built-up	20	161	141	705.00%
Fallow Land	135	7	-128	-94.81%
Agriculture	132	110	-22	-16.67%
Dense Forest	101	126	25	24.75%

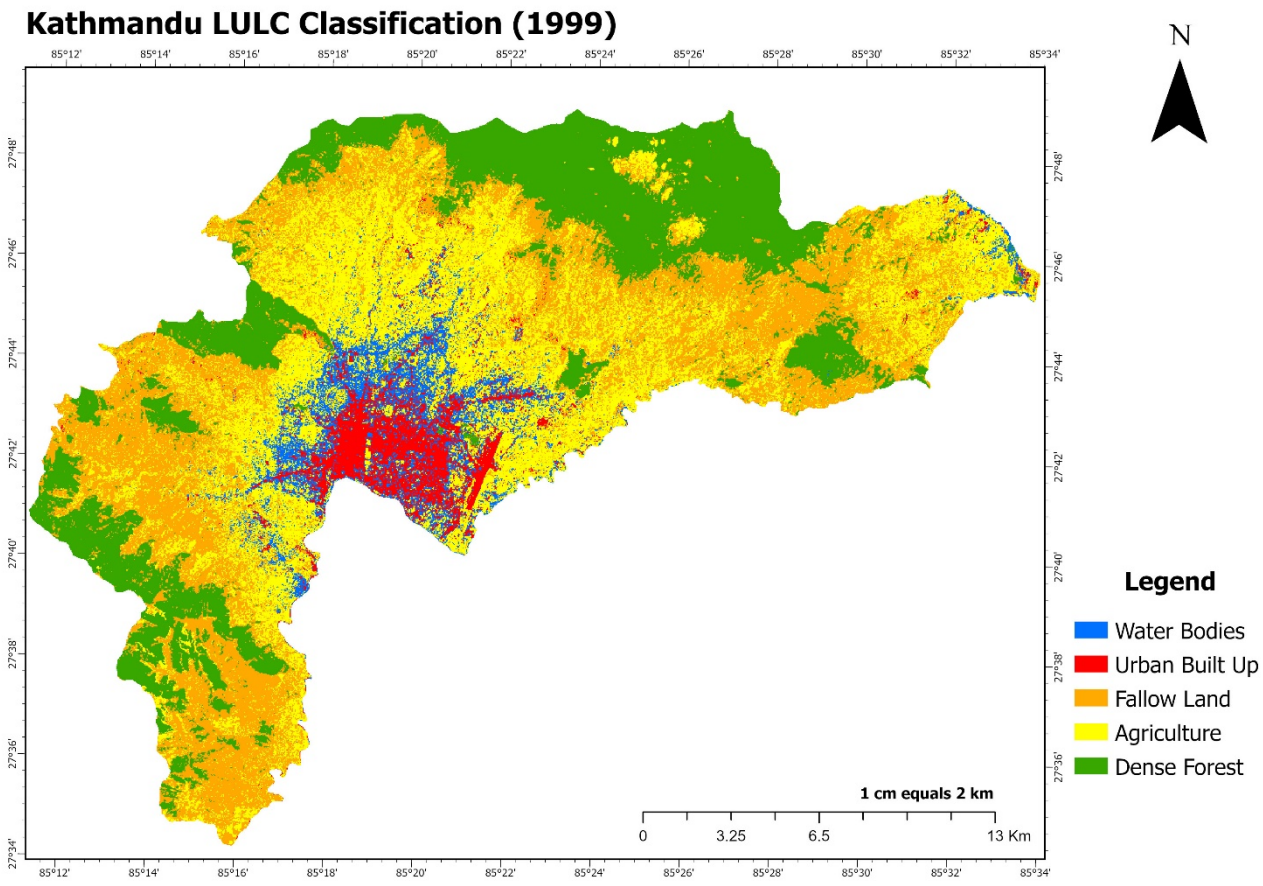

Figure 3: Classified LULC product of Kathmandu city in 1999.

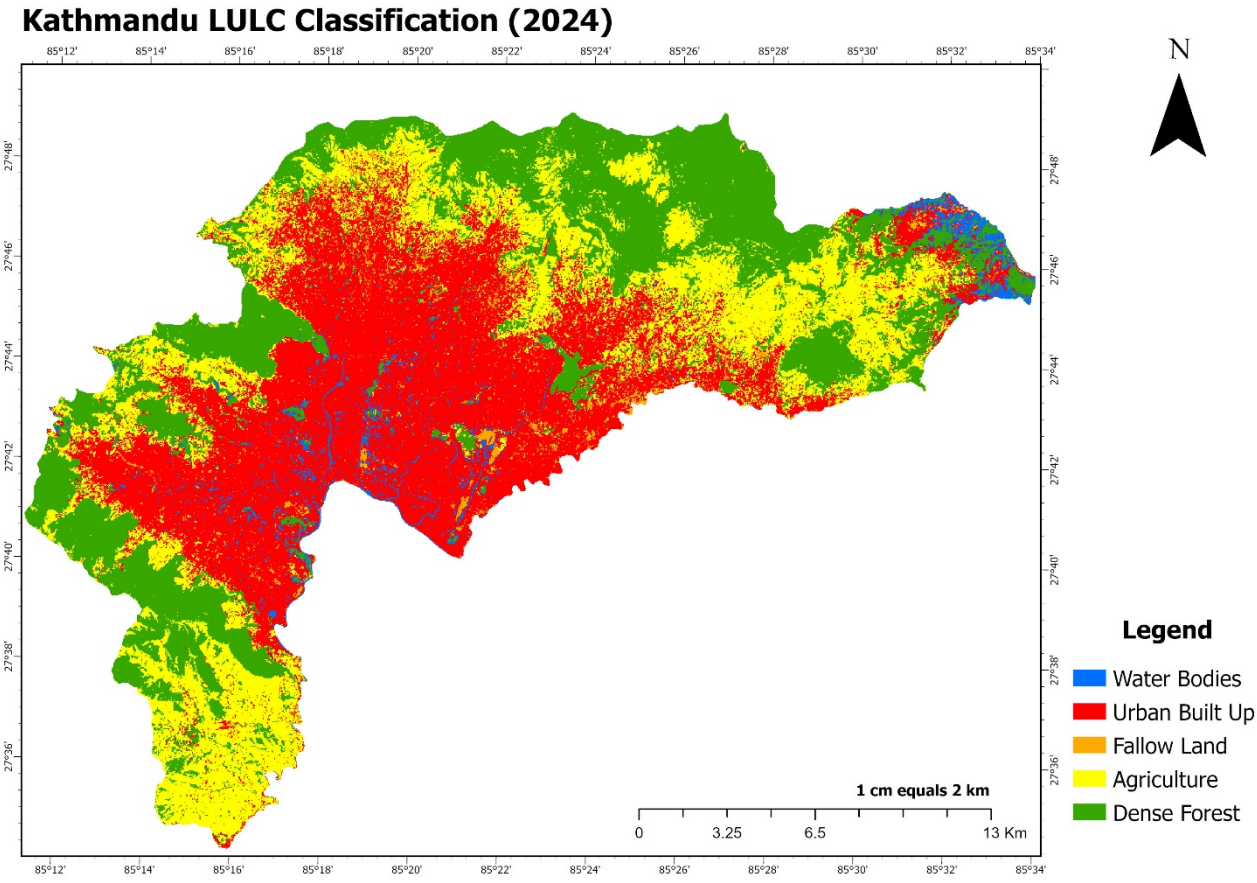

Figure 4: Classified LULC product of Kathmandu city in 2024.

3.3 Accuracy Assessment

The findings shown in table 1 and 2 demonstrate the accuracy and validation of classification results from the year 1999 and 2024 of Kathmandu city. The overall classification accuracy for the year 1999 is 81.77% and 84.90% for 2024. The comprehensive cross-validation performed against high resolution imagery on Goggle Earth Engine (GEE) revealed uniform and consistent high accuracy values for all LULC classes affirming quality and reliability of the results.

Table 5: Ground Truth validation of LULC classification Accuracy metrics for 1999 results

1999 Classified Class	Water Bodies	Urban Built Up	Fallow Land	Agriculture	Dense Forest	Total	User's Accuracy
Water Bodies	3	5	1	1	1	11	27.27%
Urban Built Up	0	9	0	0	1	10	90.00%
Fallow Land	0	0	40	12	7	59	67.80%
Agriculture	0	1	0	52	4	57	91.23%
Dense Forest	0	0	0	0	44	44	100.00%
Total	3	15	41	65	57	181	
Producer's Accuracy	100.00%	60.00%	97.56%	80.00%	77.19%		
							Overall Accuracy 81.77%

Table 6: Ground Truth validation of LULC classification Accuracy metrics for 2024 results

2024 Classified Class	Water Bodies	Urban Built Up	Fallow Land	Agriculture	Dense Forest	Total	User's Accuracy
Water Bodies	3	1	0	4	2	10	30.00%
Urban Built Up	0	58	1	10	0	69	84.06%
Fallow Land	0	1	7	2	0	10	70.00%
Agriculture	0	0	3	40	5	48	83.33%
Dense Forest	0	0	0	0	55	55	100.00%
Total	3	60	11	56	62	192	
Producer's Accuracy	100.00%	96.67%	63.64%	71.43%	88.71%		
							Overall Accuracy 84.90%

3.4 Linear Regression Results and Future projections

The statistical analysis shows urbanization has experienced a 705% growth between 1999 and 2024 with an annual increment of 5.64% km²/year. This trend in urban built-up is projected to reach 187

km² by 2030. Likewise, fallow land appears to have a catastrophic reduction by 94.81% indicating a -5.12 km²/year annually and projected to completely disappear by 2030. Water bodies face a 60% reduction with an annual decrease of -0.6 km²/year and projected to shrink by 6 km². Moreover, agricultural land reveal 16.67% decrease where its decreasing -0.88 km²/year also projected to reach 99.92 km²/year. Dense forest appears to show positive trend as it possesses 24.75% increment where its annually growing +1.0 km²/year and projected to reach 132 km²/year by the end of 2030.

Table 7: Statistical assessment of LULC change rates in Kathmandu using Linear regression model.

Land Use Class	1999 (km²)	2024 (km²)	Rate of Change (km²/year) Slope (m)	Y-intercept (b)	Regression Formula	2030 Projection (km²)
Water Bodies	25	10	-0.60	1224.00	y = -0.6x + 1,224	6
Urban Built-up	20	161	+5.64	-11,247.36	y = 5.64x - 11,247.36	195
Fallow Land	135	7	-5.12	10,367.88	y = -5.12x + 10,367.88	-23*
Agriculture	132	110	-0.88	1,889.68	y = -0.88x + 1,889.68	104
Dense Forest	101	126	1.00	-1,897.00	y = x - 1,897	133

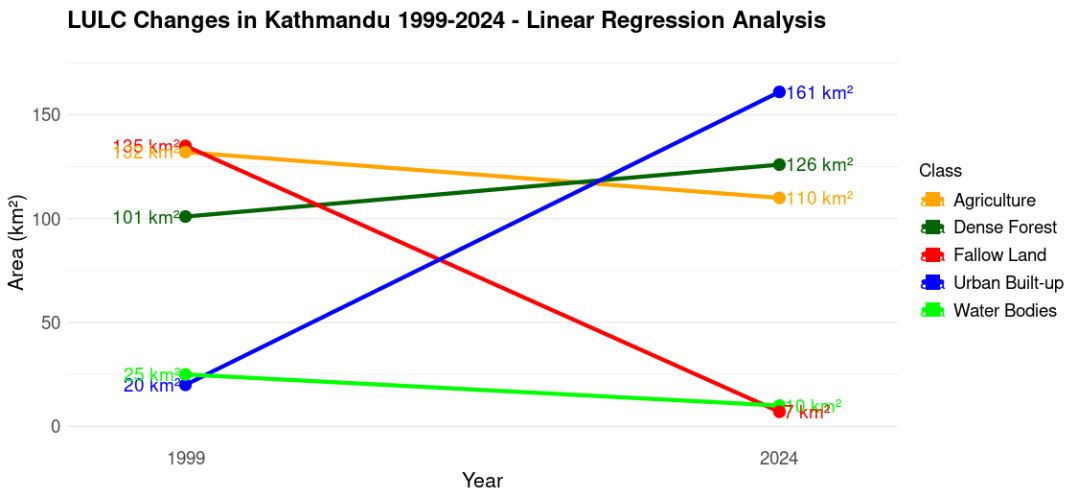

Figure 5: LULC transitions in Kathmandu based on all 5 classified classes from the year 1999 to 2024.

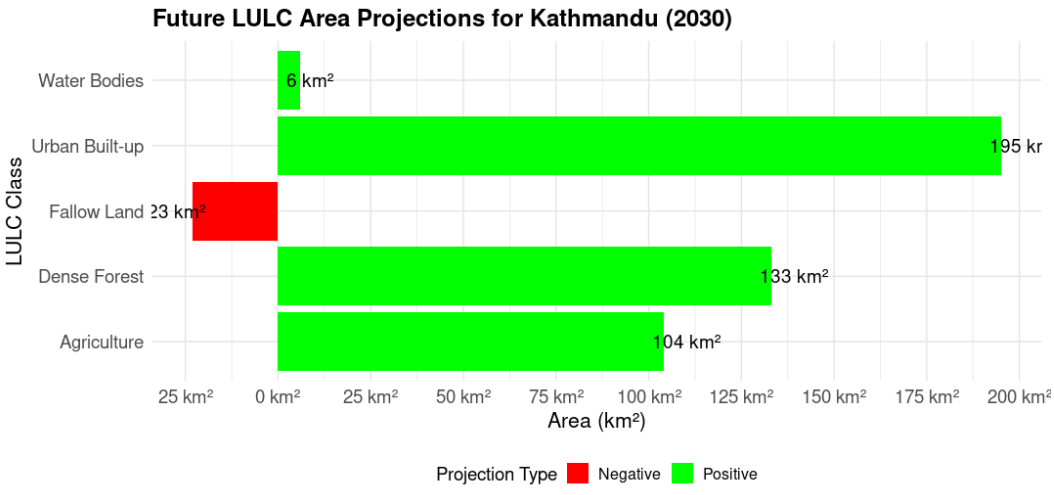

Figure 6: The horizontal bar-chart illustrates projected change of Kathmandu by the year 2030. Each length of bar shows corresponding quantified positive(growth) or negative(decline) of LULC class categories.

3.5 Challenges and Future Considerations

Although the classification findings revealed significant changes in LULC change across Kathmandu. There were technical challenges specifically while distinguishing urban built-up from fallow lands. This could potentially be due to use of 30m resolution Landsat data. Studies also suggest that fallow land mostly known for bare soil or resting agricultural land reveal similar spectral signatures to urban areas specially under dry seasons or when vegetation is dormant resulting in higher reflectance under visible and NIR (Lu et al., 2006; Zhang et al., 2006). Therefore, the areas within the city composed of bricks, concretes or bare soil could have shown similar characteristics because of the reflective properties (Small et al., 2006; Zhang et al., 2007). This overlap between signatures can be prevented by using high resolution image data with sensors capable of differentiating small urban features specially in a strategic topographical area such as Kathmandu. Therefore, if these approaches are considered, the likelihood of detecting accurate change can further enhance the reliability and strengthen the value of outcomes.

References

Derdouri, A., Wang, R., Murayama, Y.,Osaragi, T. (2021) 'Understanding the links between LULC changes and SUHI in cities: Insights from two-decadal studies (2001–2020)', Remote Sensing, 13(18), p. 3654. doi:10.3390/rs13183654.

Dutta, D., Gupta, S., Kishtawal, C.M. (2018) 'Linking LULC change with urban heat islands over 25 years: A case study of the urban-industrial city Durgapur, Eastern India', Journal of Spatial Science, 65(3), pp. 501–518. doi:10.1080/14498596.2018.1537198.

Fenta, A.A., Yasuda, H., Haregeweyn, N., Belay, A.S., Hadush, Z., Gebremedhin, M.A.,Mekonnen, G. (2017) 'The dynamics of urban expansion and land use/land cover changes using remote sensing and spatial metrics: The case of Mekelle City of northern Ethiopia', International Journal of Remote Sensing, 38(14), pp. 4107–4129. doi:10.1080/01431161.2017.1317936

González-Sanpedro, M.C., Le Toan, T., Moreno, J., Kergoat, L.,Rubio, E. (2008) 'Seasonal variations of Leaf Area Index of Agricultural Fields retrieved from Landsat Data', Remote Sensing of Environment, 112(3), pp. 810–824. doi:10.1016/j.rse.2007.06.018

Hailu, A., Mammo, S., Kidane, M. (2020) 'Dynamics of land use, land cover change trend and its drivers in Jimma Geneti District, Western Ethiopia', Land Use Policy, 99, p. 105011. doi:10.1016/j.landusepol.2020.105011.

Jarnagin, S.T. (2004) 'Regional and global patterns of population, land use, and land cover change: An overview of stressors and impacts', GIScience & Remote Sensing, 41(3), pp. 207–227. doi:10.2747/1548-1603.41.3.207.

Khamphilung, P., Konyai, S., Slack, D., Chaibandit, K., Prasertsri, N. (2023) 'Flood event detection and assessment using Sentinel-1 SAR-C time series and machine learning classifiers impacted on agricultural area, Northeastern, Thailand', International Journal of Geoinformatics, 19(6). doi:10.52939/ijg.v19i6.2691.

Lu, D.,Weng, Q. (2006) 'Use of impervious surface in urban land-use classification', Remote Sensing of Environment, 102(1–2), pp. 146–160. doi:10.1016/j.rse.2006.02.010.

Mahmoudzadeh, H., Abedini, A., Aram, F. (2022) 'Urban growth modeling and land-use/land-cover change analysis in a metropolitan area (case study: Tabriz)', Land, 11(12), p. 2162. doi:10.3390/land11122162.

Muriithi, F.K. (2016) 'Land use and land cover (LULC) changes in semi-arid sub-watersheds of Laikipia and Athi River basins, Kenya, as influenced by expanding intensive commercial horticulture', Remote Sensing Applications: Society and Environment, 3, pp. 73–88. doi:10.1016/j.rsase.2016.01.002.

Morfitt, R., Barsi, J., Levy, R., Markham, B., Micijevic, E., Ong, L., Scaramuzza, P.,Vanderwerff, K. (2015) 'Landsat-8 operational land imager (OLI) radiometric performance on-orbit', Remote Sensing, 7(2), pp. 2208–2237. doi:10.3390/rs70202208

Muhammad, R., Zhang, W., Abbas, Z., Guo, F.,Gwiazdzinski, L. (2022) 'Spatiotemporal change analysis and prediction of future land use and land cover changes using QGIS MOLUSCE plugin and Remote Sensing Big Data: A case study of Linyi, China', Land, 11(3), p. 419. doi:10.3390/land11030419.

Nichol, J. E., (1994), 'A GIS-based approach to microclimate monitoring in Singapore's high-rise housing estates'. Photogrammetric Engineering and Remote Sensing, 60, 1225–1232.

Paudyal, Y.R., Yatabe, R., Bhandary, N.P. Dahal, R.K. (2013) 'Basement topography of the Kathmandu Basin using microtremor observation', Journal of Asian Earth Sciences, 62, pp. 627–637. doi:10.1016/j.jseaes.2012.11.011

Rogan, J.,Chen, D. (2004) 'Remote Sensing Technology for mapping and monitoring land-cover and land-use change', Progress in Planning, 61(4), pp. 301–325. doi:10.1016/s0305-9006(03)00066-7.

Ross, J.L., Blangero, J., Goldstein, M.C.,Schuler, S. (1986) 'Proximate determinants of fertility in the Kathmandu Valley, Nepal: An anthropological case study', Journal of Biosocial Science, 18(2), pp. 179–196. doi:10.1017/s0021932000016114

Roy, P.S., Ramachandran, R., Paul, O., Thakur, P.K., Ravan, S.A., Behera, M.D., Sarangi, C, Kanawade, V.P., (2022) 'Anthropogenic land use and land cover changes—a review on its environmental consequences and climate change'. Journal of the Indian Society of Remote Sensing, 50(8), pp.1615-1640. doi:10.1007/s12524-022-01569-w

Seto, K.C., Güneralp, B.,Hutyra, L.R. (2012) 'Global forecasts of urban expansion to 2030 and direct impacts on biodiversity and carbon pools', Proceedings of the National Academy of Sciences, 109(40), pp. 16083–16088. doi:10.1073/pnas.1211658109.

Small, C., Lu, J.W.T. (2006) 'Estimation and vicarious validation of urban vegetation abundance by spectral mixture analysis', Remote Sensing of Environment, 100(4), pp. 441–456. doi:10.1016/j.rse.2005.10.023.

Subedi, B.P., (2014) 'Urbanization in Nepal: Spatial pattern, social demography and

development'. Population monograph of Nepal, 3, pp.95-154.

Thapa, R.B., Murayama, Y. (2010) 'Drivers of urban growth in the Kathmandu Valley, Nepal: Examining the efficacy of the analytic hierarchy process', Applied Geography, 30(1), pp. 70–83. doi:10.1016/j.apgeog.2009.10.002.

Timsina, N.P., Shrestha, A., Poudel, D.P.,Upadhyaya, R. (2020) 'Trend of urban growth in Nepal with a focus in Kathmandu Valley: A review of processes and drivers of change'. doi:10.7488/era/722

Weng, Q. (2001) 'A remote sensing–GIS evaluation of urban expansion and its impact on surface temperature in the Zhujiang Delta, China', International Journal of Remote Sensing, 22(10), pp. 1999–2014. doi:10.1080/01431160152043676.

Zurick, D. (2010) 'Kathmandu (Kathmandu Valley, Nepal; 1975–2010)', Journal of Cultural Geography, 27(3), pp. 367–378. doi:10.1080/08873631.2010.520924.

Zhang, C., Li, W.,Travis, D. (2007) 'Gaps-fill of slc-off landsat ETM+ satellite image using a geostatistical approach', International Journal of Remote Sensing, 28(22), pp. 5103–5122. doi:10.1080/01431160701250416.